Journal of Fluorescence (2019) 29:307–318
https://doi.org/10.1007/s10895-018-02340-6

ORIGINAL ARTICLE

Spectroscopic Evaluation of Novel Adenine/Thymine-Conjugated Naphthalenediimides: Preference of Adenine-Adenine over Thymine-Thymine Intermolecular Hydrogen Bonding in Adenine- and Thymine-Functionalized Naphthalenediimides

Digambara Patra[1] · Nadine Al Homsi[1] · Sara Jaafar[1] · Zeina Neouchy[1] · Jomana Elaridi[2] · Ali Koubeissi[1] · Kamal H. Bouhadir[1]

Received: 26 September 2018 / Accepted: 26 December 2018 / Published online: 4 January 2019

Abstract

The synthesis and spectroscopic characterization of novel nucleobase (adenine/thymine)-conjugated naphthalenediimides (NDIs), namely, NDI-AA, NDI-TT, and NDI-AT have been successfully achieved. NDI-AA, NDI-TT and NDI-AT have similar absorption in the 300–400 nm region. The effect of solvent on the absorption spectrum indicates aggregation, either through intermolecular π-σ interaction among the main chromophore or through intermolecular hydrogen bonding between adenine and adenine group. Addition of water does not assist hydrogen bond formation between thymine-thymine, rather increasing the polarity of the solvent encourages π-σ interaction among NDI-TTs. No spectral change for NDI-TT with increasing temperature confirms hydrogen bonding is not playing a crucial role in NDI-TT. A fluorescence study on NDI-AA also establishes excimer formation along with ground state aggregation. As the water content in the solvent mixture increases, aggregation of NDI-AA is discouraged due to adenine-adenine hydrogen bonding in accordance with earlier results. At the same time, the NDI-TT emission spectrum does not shift to the blue region and the intensity of the peak around 535 nm increases at the expense of fluorescence in 411 nm. Thus, increasing water content in the solvent mixture facilitates aggregation through π-σ interaction in NDI-TT as thymine-thymine hydrogen bonding is less pronounced.

Keywords Naphthalenediimide · Adenine · Thymine · Absorption · Fluorescence · Hydrogen bonding

Introduction

The design of supramolecular structures often incorporates aromatic molecules because spectroscopic and redox properties of aromatic molecules can be easily predicted [1]. Application of naphthalenediimides (NDIs) in supramolecular and materials chemistry has been extensively reported and reviewed in the literature for synthesis of new materials [1–5]. In many cases, NDI derivatives have demonstrated potential use in the field of molecular sensors [6–8] and in conducting films [9, 10]. These molecules can self-assemble and intercalate in larger multicomponent complexes [1, 11]. NDI self-assembly is facilitated by hydrogen bonding and π-π stacking [12]. NDI derivatives may have future applications in the biomedical field due to their gelling properties and high versatility [1, 5, 6, 8]. Attempts to expand the family of NDIs through functionalization of the naphthalene core or the diimide nitrogens have resulted in a variety of molecules with diverse absorption and emission properties [1, 13].

Attempts to design self-organizing NDI derivatives have included the synthesis of adenine and thymine functionalized NDIs [14]. This idea was inspired by the compelling ability of nucleobases, the building blocks of deoxyribonucleic acid (DNA) and ribonucleic acid (RNA), to form hydrogen-

Electronic supplementary material The online version of this article (https://doi.org/10.1007/s10895-018-02340-6) contains supplementary material, which is available to authorized users.

✉ Digambara Patra
dp03@aub.edu.lb

✉ Kamal H. Bouhadir
kb05@aub.edu.lb

[1] Department of Chemistry, American University of Beirut, P.O. Box 11-0236, Beirut, Lebanon

[2] Department of Natural Sciences, Lebanese American University, P.O. Box 13-5053, Beirut, Lebanon

bonded molecular assemblies. Adenine-NDI-Adenine (NDI-AA) and Thymine-NDI-Thymine (NDI-TT) have been successfully synthesized and shown to self-assemble on templates of peptide nucleic acid (PNA) dimers whose role is to mimic the nucleobases [14]. Complexes with a greater affinity have been observed compared to the self-assembly of non-conjugated nucleobases on a PNA template [3]. Furthermore, the NDI-nucleobases self-assemble in a unique and well-defined manner on the PNA templates [3]. NDI-AA conjugates assemble into nanoribbons while with complementary PNA-TT templating, 2D-microstructures have resulted. For the NDI-TT conjugated, it has self-organized into porous spheres whereas complementary PNA-AA templating have resulted in fibers and petal-like 2D sheets [3]. Hence, the difference in the strength of self-assembly has reflected by a change in the resulted nanostructures [12, 14, 15].

In this paper, we report the synthesis and photophysical properties of novel nucleobase-functionalized NDIs, specifically NDI-AA and NDI-TT. The purity of the final product was assessed, and the structure was elucidated using ^{1}H-NMR, ^{13}C-NMR, DEPT, COSY, NOESY, FT-IR, and MS. The collected data confirmed the chemical structures of all the products in this study. In addition, extensive photophysical properties for NDI-AA and NDI-TT were realized in different solvents and at various proportions.

Experimental

Instrumentation Melting points were determined on a Fisher-Johns apparatus and were uncorrected. NMR spectra were determined in deuterated solvents with TMS as the internal standard on a Bruker AM 300 NMR spectrometer. Chemical shifts are reported in ppm (δ) downfield relative to TMS. Infrared spectra were recorded as KBr pellets using a Nicolet AVATAR 360 FTIR ESP spectrometer with a Hewlett Packard Desk jet 840C plotter.

Attenuated total reflectance Fourier transform infrared (ATR-FTIR) spectrometry was performed on dry samples. ATR-FTIR spectra (4 scans, 4 cm^{-1} resolution, wave number range 4000–650 cm^{-1}) were obtained using a Perkin Elmer FTIR Spectrum 2000 Spectrophotometer with a diamond/ZnSe crystal window. All spectra were recorded under ambient conditions. SPECTRUM software (Perkin Elmer) was used for data collection. The IR bands are reported in wavenumbers (cm^{-1}). Thin layer chromatography (TLC) was performed on polygram Sil G/UV_{254} silica gel sheets. The absorption spectra were recorded at room temperature using a JASCO V-570 UV–VIS–NIR spectrophotometer. The concentration used for absorption measurement was 100 μM. The fluorescence measurements were documented with resolution increment 1 nm and slit 5 nm using Jobin-Yvon-Horiba Fluorolog III fluorometer and the FluorEssence program. The excitation source was a 100 W Xenon lamp, and the detector used was R-928 operating at a voltage of 950 V. The concentration used for fluorescence measurement was 10 μM.

Preparative column chromatography employed ACROS silica gel (60 Å, 200–400 mesh). Preparative thin layer chromatography employed ALLTECH silica gel 60 F_{254} plates. Reagents used in the syntheses were purchased from the Aldrich Chemical Company (Milwaukee, WI, USA), ACROS Chemicals (Belgium), Fisher Scientific Company (Fair Lawn, NJ, USA), and were used as received.

Synthesis 1-(2-(Carboxyethyl)ethyl)thymine (**2**): Thymine **1** (2.00 g, 16 mmol) was dissolved in an ethanol:benzene mixture (8:1, 60 mL) in the presence of a catalytic amount of sodium metal (33 mg) and ethyl acrylate (2.2 mL, 20 mmol) was added dropwise after hydrogen evolution ceased. The mixture was heated at reflux overnight and subsequently concentrated under reduced pressure. The flask was immersed in an ice-water bath and the resultant precipitate was filtered, washed with cold ethanol and dried under reduced pressure to afford **2** as a colorless solid (3.10 g, 86%). Mp: 167–168 °C; ^{1}H NMR (300 MHz, $CDCl_3$): δ 1.25 (t, J = 6.9 Hz, 3H), 1.91 (s, 3H), 2.77 (t, J = 6.0 Hz, 2H), 3.95 (t, J = 6.0 Hz, 2H), 4.15 (q, J = 7.1 Hz, 2H), 7.21 (s, 1H), 9.41 (bs, 1H); ^{13}C NMR (75 MHz, $CDCl_3$): δ 12.2, 14.1, 33.1, 45.0, 61.1, 110.2, 141.6, 150.6, 164.1, 171.4. The spectroscopic data are in agreement with those reported in the literature [16].

1-(2-Hydrazidoethyl)thymine (**3**): Thymine-ester **2** (3.50 g, 15.4 mmol) was dissolved in ethanol (77 mL) followed by dropwise addition of hydrazine monohydrate ($N_2H_4.H_2O$, 2.3 mL, 46.2 mmol) and the resulting mixture was heated at reflux overnight. The solvent was evaporated to dryness under reduced pressure and the solid was triturated in cold ethanol and filtered to afford **3** as a colorless solid (2.84 g, 86%). Mp: 188–190 °C; FT-IR (ATR, cm^{-1}): 1224,1636, 1662, 3347; ^{1}H NMR (300 MHz, D_2O): δ 1.86 (s, 3H), 2.58 (t, J = 6.4 Hz, 2H), 4.00 (t, J = 6.3 Hz, 2H), 7.42 (s, 1H); ^{13}C NMR (75 MHz, D_2O): δ 14.1, 35.6, 48.2, 113.6, 145.9, 154.9, 169.9, 174.6. The spectroscopic data are in agreement with those reported in the literature [16].

NDI-TT (**4**): 1,4,5,8-Naphthalenetetracarboxylic dianhydride (0.5, 1.86 mmol) was added to a solution of thymine-hydrazide **3** (0.794 g, 3.72 mmol) in DMF (20 mL). The resulting mixture was heated at 110 °C for 6 days. The reaction mixture was cooled to room temperature and the precipitate was filtered and washed with ethanol. The solid was triturated with hot ethanol (20 mL), filtered and washed with ethanol. The product was dried under reduced pressure at 80 °C for 2 days to furnish **4** as a pale yellow solid (0.89 g, 79%). Mp: 333–336 °C; FT-IR (KBr, cm^{-1}): 1250, 1668, 1692; ^{1}H NMR (300 MHz, DMSO): 1.76 (s, 6H), 2.84 (t,

J = 6 Hz, 4H), 3.95 (t, J = 6 Hz, 4H), 7.49 (s, 2H), 8.75 (s, 4H), 11.06 (d, J = 8 Hz, 2H), 11.31 (bs, 2H);**);** ^{13}C NMR (75 MHz, D_2O): δ 12.1, 32.2, 44.2, 108.2, 126.3, 126.5, 131.4, 131.4, 142.1, 150.9, 160.7, 164.5, 169.1; Mass spectrum (ESI$^-$): *m/z* [M-H$^+$] calcd for $C_{30}H_{23}N_8O_{10}$: 655.1, found 655.0.

1-(2-(Carboxyethyl)ethyl)adenine (**6**): Adenine **5** (16.7 g, 0.123 mol) was dissolved in an ethanol:benzene mixture (8:1, 562 mL) and the flask was immersed in an ice-water bath. Sodium metal (175 mg) was carefully added followed by the dropwise addition of ethyl acrylate (5 mL) and the mixture was refluxed overnight. The solvent was evaporated under reduced pressure and the residue was triturated with cold ethanol, filtered and dried under reduced pressure to afford the ester **6** as a colorless solid (26.7 g, 92%). Mp: 167–168 °C; FT-IR (KBr, cm^{-1}): 1204, 1481, 1609, 1733, 3315; ^{1}H NMR (300 MHz, DMSO): 1.12 (t, J = 7.1 Hz, 3H), 2.94 (t, J = 6.8 Hz, 2H), 4.03 (q, J = 7.2 Hz, 2H), 4.38 (t, J = 6.8 Hz, 2H), 7.24 (s, 2H), 8.11 (s, 1H), 8.14 (s, 1H); ^{13}C NMR (75 MHz, DMSO): 13.8, 33.6, 38.6, 60.2, 118.6, 140.9, 149.4, 152.3, 155.9, 170.5. The spectroscopic data are in agreement with those reported in the literature [16].

1-(2-Hydrazidoethyl)adenine (**7**): Hydrazine-hydrate (9.58 g, 191 mmol) was added dropwise to a stirred solution of **6** (15.0 g, 63.7 mmol) in ethanol (300 mL) at room temperature. The mixture was then heated at reflux for 24 h. The solution was cooled down to room temperature and the solvent was removed under reduced pressure. The residue was triturated with cold ethanol, filtered and dried under reduced pressure to afford the hydrazide **7** as a colorless solid (13.9 g, 99%). Mp: 268–271 °C; FT-IR (ATR, cm^{-1}): 1298, 1647, 3160, 3326; ^{1}H NMR (300 MHz, $D_2O + D_2SO_4$): 3.05 (t, J = 6.5 Hz, 2H), 4.68 (t, J = 6.4 Hz, 2H), 8.41 (s, 1H), 8.47 (s, 1H); ^{13}C NMR (75 MHz, D_2O): δ 35.3, 42.5, 120.5, 147.0, 147.5, 151.1, 152.3, 172.9. The spectroscopic data are in agreement with those reported in the literature [16].

NDI-AA (**8**): 1,4,5,8-Naphthalenetetracarboxylic dianhydride (0.50 g, 1.86 mmol) was added to a solution of 1-(2-hydrazidoethyl)adenine **7** (0.822 g, 3.72 mmol in DMF (20 mL). and the resulting mixture was heated at 130 °C for 6 days. The reaction mixture was cooled to room temperature and the precipitate was filtered and washed with ethanol. The solid was triturated with 20 mL of hot ethanol, filtered and washed with cold ethanol. The product was dried under reduced pressure at 80 °C for two days to afford a brown solid (0.962 g, 77%). Mp: 305–310 °C; FT-IR (KBr, cm^{-1}): 1695, 1669, 1250; ^{1}H NMR (300 MHz, DMSO): 3.06 (t, J = 6 Jz, 4H), 4.46 (t, J = 6 Hz, 4H), 7.25 (s, 2H), 8.09 (s, 2H), 8.18 (s, 2H), 8.75 (s, 4H), 11.05 (s, 1H), 11.10 (s, 1 H); ^{13}C NMR (75 MHz, $CDCl_3$): 32.8, 35.7, 113.5, 117.9, 126.2, 131.3, 144.3, 148.4, 149.8, 158.4, 159.0, 160.4, 168.6. Mass spectrum (ESI$^-$): *m/z* [M-H$^+$] calcd for $C_{30}H_{21}N_{14}O_6$: 673.2, found.

NMI-A (**9**): A solution of 1,4,5,8-naphthalenetetracarboxylic dianhydride (0.64 g, 2.40 mmol) was prepared with water (41 mL) and KOH (1.5 M, 46 mL). The pH of this solution was adjusted to 5.6 with acetic acid (2 M, ~30 mL). Adenine hydrazide **7** (0.60 g, 2.90 mmol) was added to this solution and the pH was adjusted again to 5.6. The cloudy light brown mixture was heated at reflux overnight and was subsequently cooled to room temperature and filtered. The filtrate was acidified to pH 1.8 and the mixture was heated at ~80 °C for 30 min. The product was dried at 80 °C under reduced pressure to yield the coupled product **9** as a dark beige powder **(**0.37 g, 32%). Mp: 315–318 °C; FT-IR (ATR, cm^{-1}): 1166, 1248, 1687; ^{1}H NMR (500 MHz, DMSO): 3.04 (t, J = 6.8 Hz, 2H), 4.46 (J = 6.8 Hz, 2H), 7.26 (s, 2H), 8.10 (s, 1H), 8.19 (s, 1H), 8.23 (d, J = 7.5 Hz, 2H), 8.61 (d, J = 7.5 Hz, 2H), 11.01 (s, 1H); ^{13}C NMR (125 MHz, DMSO): 32.9, 39.1, 124.4, 126.1, 128.8, 129.9, 131.5, 137.8, 141.0, 143.9, 147.1, 149.2152.0, 159.3, 161.3, 168.8. Mass spectrum (ESI$^-$): *m/z* [M-H$^+$] calcd for $C_{22}H_{14}N_7O_7$: 488.1, found.

NMI-T (**11**): A solution of 1,4,5,8-naphthalenetetracarboxylic dianhydride (3.75 g, 14 mmol) was prepared with water (245 mL) and KOH (1.5 M, 276 mL). The pH of the solution was adjusted to 5.6 with acetic acid 2 M (~170 mL). Thymine hydrazide **3** (3.00 g, 14 mmol) was added to this solution and the pH was adjusted again to 5.6. The brown mixture was heated at reflux overnight and was subsequently cooled to room temperature and filtered. The filtrate was acidified to pH 1.8 and the light brown mixture was heated at ~80 °C for 30 min. The product was dried at 80 °C under reduced pressure to yield the coupled product **11** as a light brown powder (6.05 g, 90%). Mp: 305–307 °C; FT-IR (ATR, cm^{-1}): 1186, 1237, 1285, 1374, 1670, 1684; ^{1}H NMR (300 MHz, DMSO + TFA): 1.77 (s, 3H), 2.81 (t, J = 6.5 Hz, 2H), 3.96 (t, J = 6.3 Hz, 2H), 7.50 (s, 1H), 8.26 (d, J = 7.5 Hz, 2H), 8.62 (d, J = 7.5 Hz, 2H), 11.04 (s, 1H), 11.32 (s, 1H); ^{13}C NMR (125 MHz, DMSO + TFA): 12.4, 32.7, 44.6, 124.6, 126.1, 128.9, 129.9, 131.4, 137.8, 142.6, 151.3, 161.3, 165.0, 168.8, 169.5. Mass spectrum (ESI$^-$): *m/z* [M-H$^+$] calcd for $C_{22}H_{15}N_4O_9$: 479.1, found.

NDI-AT (**10**): In a sealed tube, a mixture of naphthalene mono-thymine-imide **11** (0.35 g, 0.7 mmol, 1 eq), adenine hydrazide (0.15 g, 0.7 mmol) and three drops of TFA in DMF (11 mL) was heated and for 6 days at 130 °C. The mixture was cooled to room temperature and filtered under reduced pressure. The precipitate was washed with ethanol and triturated with hot ethanol. The product was dried at 80 °C under reduced pressure to yield NDI-AT **10** as a dark grey powder (0.23 g, 53%). Mp: >355 °C. FT-IR (ATR, cm^{-1}): 1200, 1243, 1355, 1449, 1476, 1657, 1690; ^{1}H NMR (300 MHz, DMSO + TFA): 1.76 (s, 3H), 2.79 (t, J = 6.6 Hz, 2H), 2.91 (t, J = 6.6 Hz, 2H), 3.94 (t, J = 6.5 Hz, 2H), 4.48–4.53 (m, 2H), 7.48 (s, 1H), 8.23 (d, J = 7.5 Hz, 2H), 8.42 (s, 1H), 8.50 (s, 1H), 8.61 (d, J = 7.8 Hz, 2H), 11.01 (s, 1H), 11.04 (s, 1H), 11.29 (s, 1H); ^{13}C NMR (125 MHz, DMSO + TFA): 12.4, 32.7, 33.1, 33.3, 44.6, 118.6, 124.6, 126.1, 126.8, 127.0, 128.8, 130.0, 131.5, 137.8, 142.6, 143.7, 147.6, 149.2,

151.3, 159.2, 161.3, 165.0, 169.1, 169.9. Mass spectrum (ESI$^-$): *m/z* [M-H$^+$] calcd for $C_{30}H_{22}N_{11}O_8$: 664.2, found.

Results and Discussion

The preparation of nucleobase-naphthalenediimide conjugates **4** (NDI-TT) and **8** (NDI-AA) are presented in Scheme 1. The novel NDI-derivatives were synthesized via a straightforward, facile and high-yielding strategy from cheap, readily available starting materials. Initially, the nucleobases thymine **1** and adenine **5** underwent Michael addition upon reaction with ethyl acrylate in ethanol in the presence of a catalytic amount of sodium metal. This led to the incorporation of a two-carbon ethylene spacer that links the nucleobase to the new ester functionality. The thymine- and adenine-derived ethyl esters **2** and **6** were isolated as solids in 86% and 92% yields respectively. Hydrazinolysis of the ethyl esters **2** and **6** in refluxing ethanol overnight furnished the nucleobase hydrazides **3** and **7** in excellent yields of 86% and 99% yields respectively. The nucleobase-hydrazides **3** and **7** were condensed with 1,4,5,8-naphthalenetetracarboxylic dianhydride (NDA) in a 2:1 mol ratio in dimethylformamide (DMF) to give the nucleobase-appended NDI-derivatives **4** and **8** in 79% and 77% yields.

The synthesized compounds were characterized by IR, ^{1}H and ^{13}C NMR spectroscopy. Spectroscopic data of the nucleobase esters **2** and **6** and acylhydrazides **3** and **7** are consistent with those previously reported in the literature [16, 17]. Briefly, the ^{1}H NMR spectra of **2** and **6** displayed signals corresponding to the methylene (δ 4.15) and methyl (δ 1.25) hydrogens of the ethyl ester group, in addition to two new triplets attributed to the newly incorporated ethylene spacer. Similarly, conversion of the esters to the hydrazides was supported by the disappearance of the ethyl hydrogens; the $NHNH_2$ protons did not appear due to exchange with the D_2O solvent. However, the IR showed C=O peaks at 1663 and 1637 cm^{-1} and an NH_2 stretch at 3347 cm^{-1}. Formation of the NDI-TT derivative **4** was supported with the appearance of a [M-H$^+$] peak at 655.0 in the mass spectrum. Furthermore, the ^{1}H NMR spectrum displayed a new aromatic signal at δ 8.75 attributed to the newly installed naphthalene core in addition to chemical shift changes of the thymine protons and the ethylene spacer. Similar observations were made in the spectroscopic analysis of NDI-AA **8:** C=O stretch at 1695 cm^{-1}, a new aromatic proton signal at δ 8.75 and two carbonyl carbon peaks at δ 160.4 and 168.6 corresponding to the hydrazide and imide carbons respectively.

Synthesis of the adenine-thymine appended naphthalenediimide conjugate **10** (NDI-AT) is outlined in Scheme 2. NDI-AT **10** can be synthesized from either the thymine **3** or adenine **7** derivative via two successive reactions between the nucleobase hydrazides and 1,4,5,8-

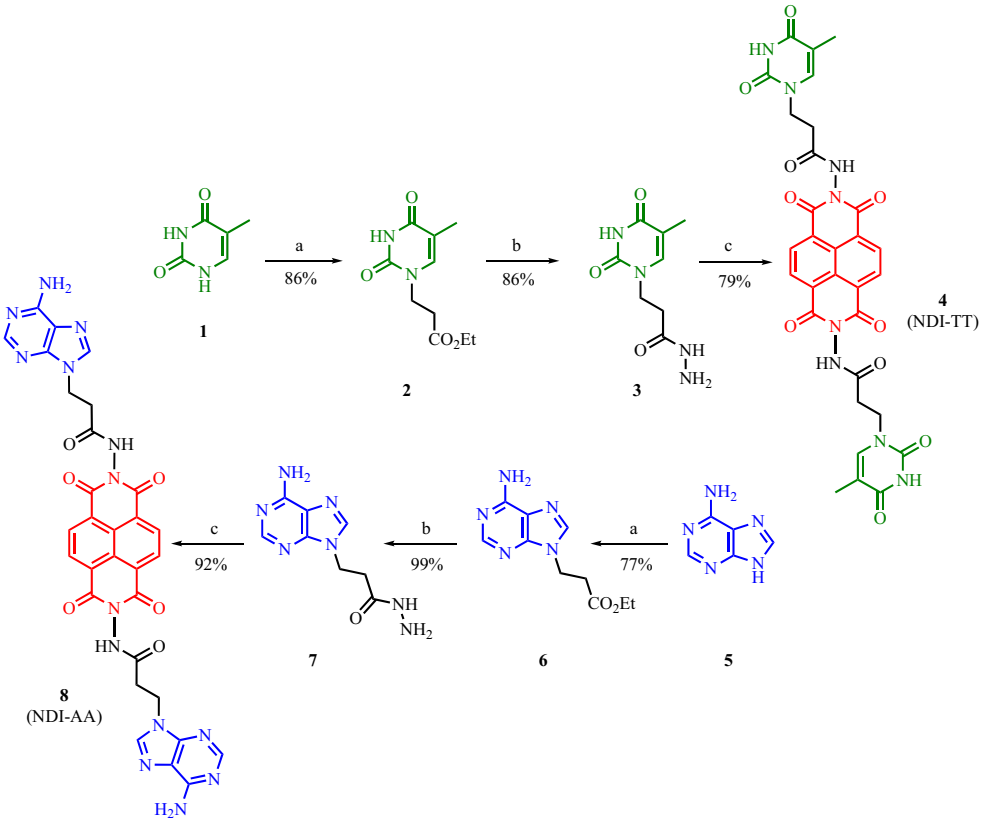

Scheme 1 Reagents and conditions: (a) Ethyl acrylate, Na, EtOH, reflux, 24 h. (b) $N_2H_4.H_2O$, EtOH, reflux, 24 h. (c) NDA, DMF, 110 °C, in sealed tube, 10–12 h

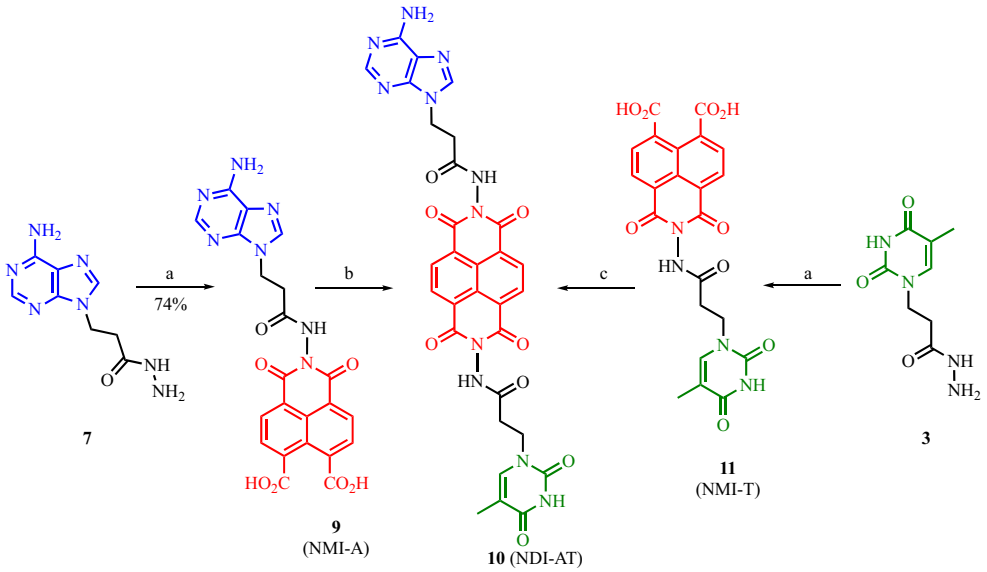

Scheme 2 Reagents and conditions: (a) NDA, KOH, H_2O, reflux, overnight. (b) **3**, TFA, 130 °C, sealed tube, 6 d. (c) **7**, TFA, 130 °C, sealed tube, 6 d

naphthalenetetracarboxylic dianhydride (NDA). For example, thymine hydrazide **7** was heated with NDA in aqueous potassium hydroxide solution overnight to afford the thymine-linked naphthalene mono-imide **11** (NMI-T) in 90% yield. The appearance of two new aromatic doublets at δ 8.23 and 8.61 in the ^{1}H NMR spectrum, characteristic of the two sets of aromatic protons in the naphthalene core, in addition to signals typical of the thymine-linker, provides evidence for formation of the coupled product. Subsequent reaction of **11** with adenine hydrazide **7** in a sealed tube at 130 °C furnished the coupled product **10** (NDI-AT) in 53% yield.

The UV-visible spectra of NDI-AA **8**, NDI-TT **4** and a 1:1 NDI-AA **8**: NDI-TT **4** mixture in 60:40% DMSO/water are presented in Fig. 1. Interestingly, NDI-AA **8** and NDI-TT **4**, and their mixture showed similar absorption in the 300–400 nm region. The vibrational peaks at around 340 nm, 358 nm and 378 nm were well resolved in all cases. Since there is no difference in positions of absorption spectra of **8** and **4** (and their mixture), the influence of adenine/thymine on the absorption of the NDI chromophore is negligible and the absorption is characteristic of π-π* transitions of NDI chromophores polarized along the z-axis [14].

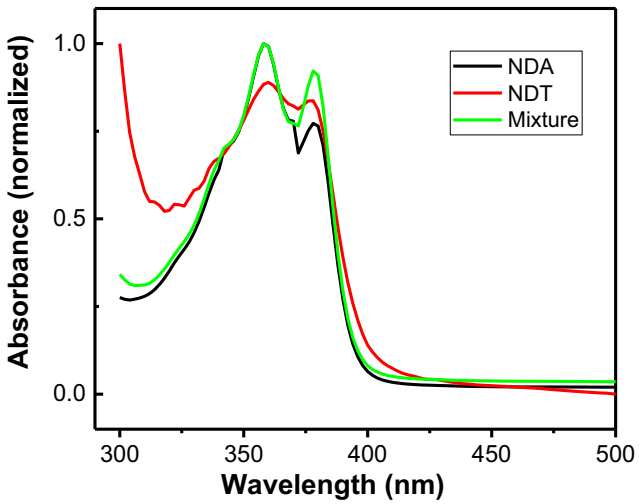

Fig. 1 UV-visible absorption spectra of NDI-AA **8**, NDI-TT **4** and their mixture in 60:40% DMSO/water

As seen in Fig. 2a, upon the addition of water in DMSO, the absorption spectrum of NDI-AA **8** showed an increase in absorbance at the maximum (at 358 nm and 378 nm) but around 400 nm and 310 nm regions, the absorbance decreased. It was also observed that as the water concentration increased, the absorption spectrum of NDI-AA **8** was found to be narrower. This observation is interesting. There are two possibilities for two NDI-AA **8** molecules to aggregate, either through intermolecular π-σ interaction between the main chromophore or through intermolecular hydrogen bonding between adenine-adenine groups. Aggregation generally decreases the absorbance of chromophores, however, depending on the aggregation type, a blue or red shift can be observed in the absorption spectrum. In this case, no additional peak was observed. However, the increase in absorbance could be due to weakening intermolecular π-σ interaction that is a result of strong hydrogen bonding between adenine-adenine groups facilitated by solvent molecules like water.

This was further examined by replacing water (protic solvent) with acetonitrile (aprotic solvent) as depicted in Fig. 2b. When acetonitrile was added in DMSO, the absorption spectrum of NDI-AA **8** showed a slight blue shift with an increase in absorption intensity. However, the absorption spectra of **8** were also found to be narrower with increasing acetonitrile concentration. The blue shift is due to low polarity of acetonitrile and increasing absorbance is due to a weakening of π-σ interaction in the relatively less polar solvent. Interestingly,

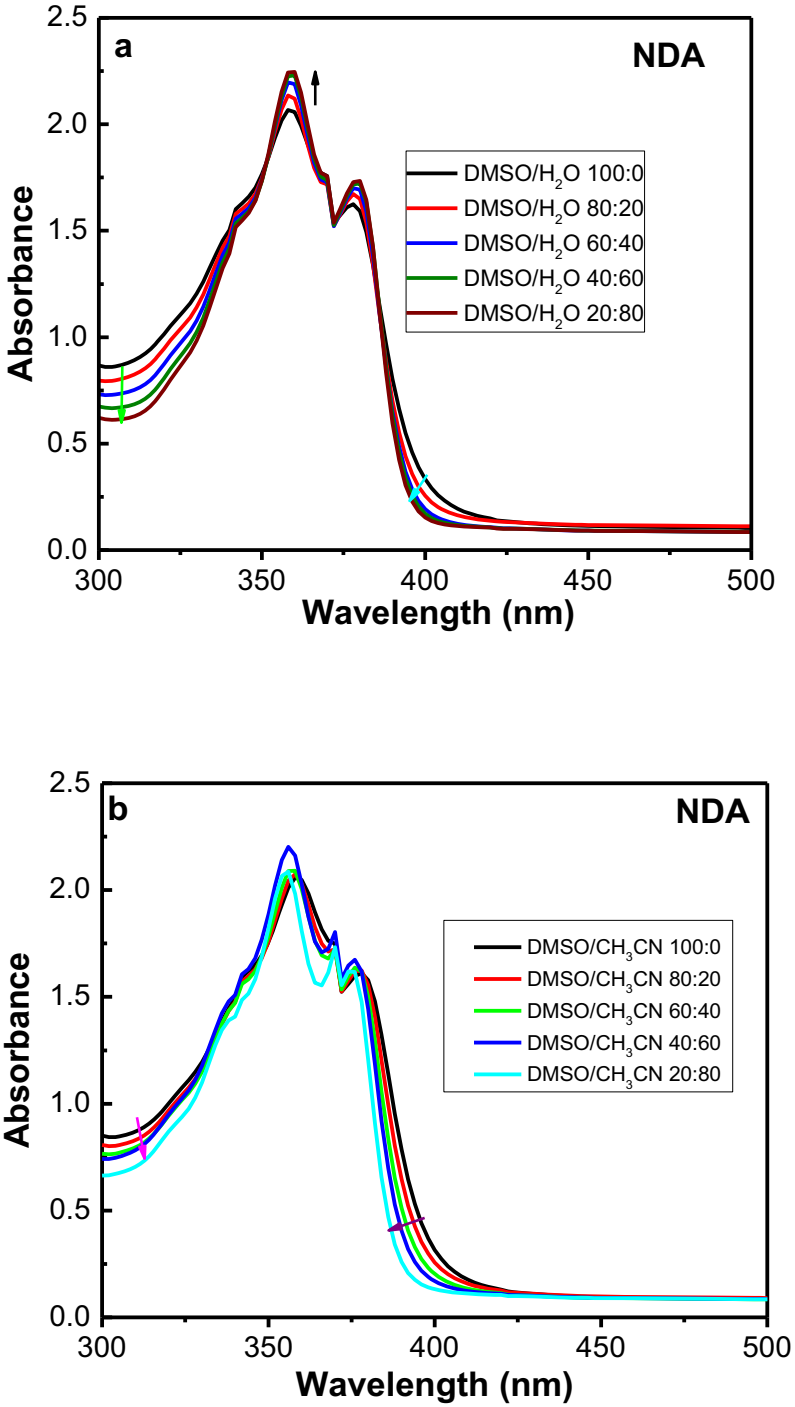

Fig. 2 UV-visible absorption spectra of NDI-AA **8** in (**a**) DMSO/water and (**b**) DMSO/acetonitrile

(Fig. 3a), the absorbance of NDI-TT **4** decreased remarkably with the addition of water in DMSO. This decrease was unexpected as the interaction of **8** and **4** was predicted to be similar. This will be discussed later on. The addition of acetonitrile to DMSO (Fig. 3b), resulted in similar observations for NDI-TT **4** and NDI-AA **8**, which was expected because hydrogen bonding does not play any role in DMSO/acetonitrile mixture. However, the absorption spectra of NDI-AT **10,** as depicted in Fig. 4a, behaved similar to NDI-AA **8** suggesting conjugated aromatic rings of adenine has a dominant effect on π-π^* transitions of NDI chromophores.

To understand different species in the ground and excited state, we recorded the more sensitive fluorescence excitation and emission spectra of NDI-AA **8** and NDI-TT **4** at different possible excitation and emission wavelengths. At excitation wavelengths 360 nm, 368 nm, 378 nm and

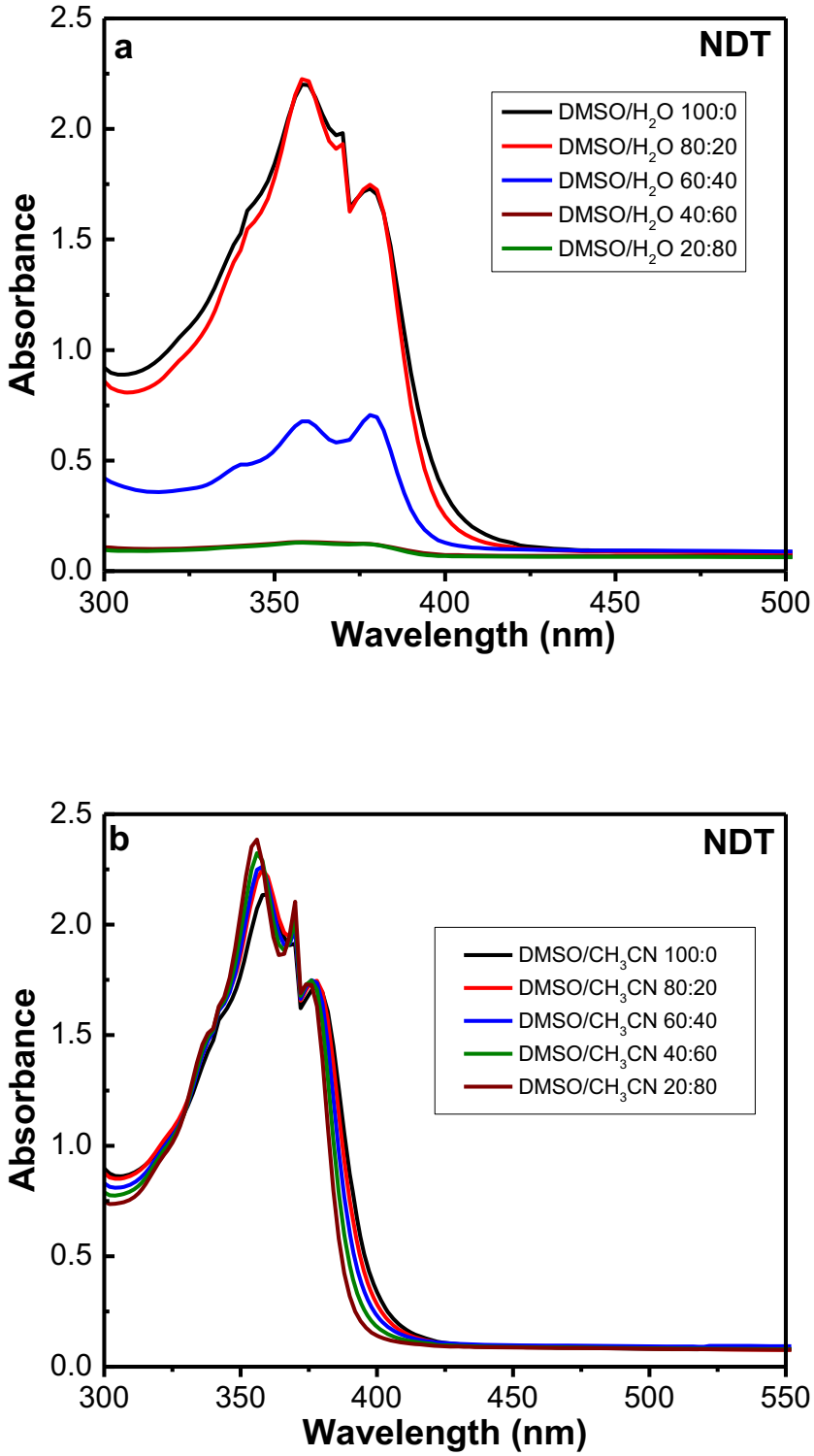

Fig. 3 UV-visible absorption spectra of NDI-TT **4** in (**a**) DMSO/water and (**b**) DMSO/acetonitrile solvent mixture

409 nm, both **8** (see Fig. 5), **4** (see Fig. 6) and **10** (see Fig. 4b) showed similar emission spectra with vibronic structures. However, the fluorescence intensity of the emission band at around 541 nm remarkably increased at excitation wavelength 409 nm. Similarly, at emission wavelengths 411 nm, 434 nm and 541 nm both NDI-AA **8** and NDI-TT **4** gave similar excitation spectra but the fluorescence intensity was remarkably high at around 405–410 nm. It should be noted that the excitation spectra and absorption spectra were different, which suggest the absorbing and emitting species are different indicating aggregation of chromophores in the excited state. The band at around

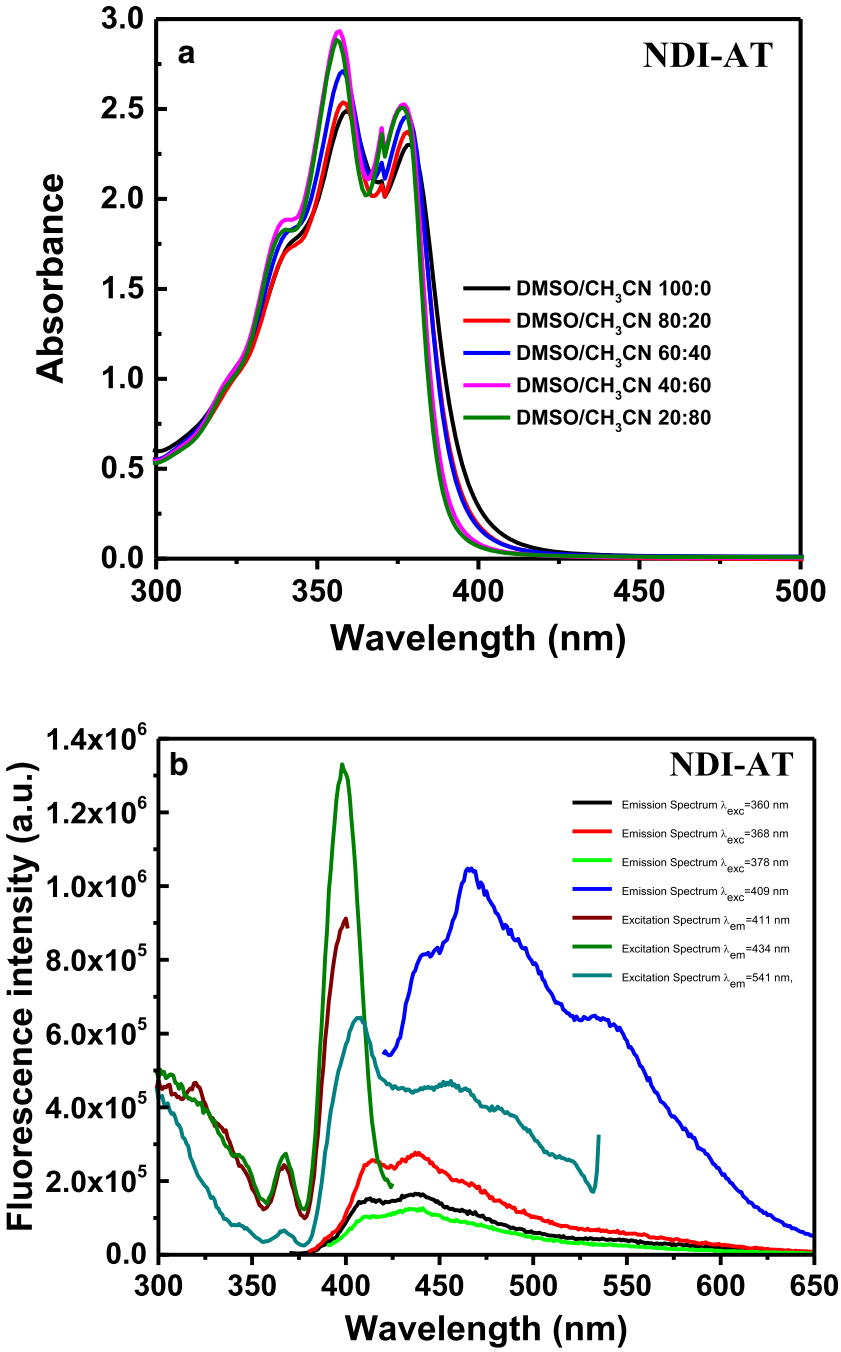

Fig. 4 **a** UV-visible absorption spectra of NDI-AT **10** in DMSO/acetonitrile mixture; **b** Fluorescence excitation and emission spectra of NDI-AT **10** in different excitation and emission wavelengths in 60:40 DMSO/water mixture

405–410 nm was not clearly observed in absorption spectra but it is well resolved in the excitation spectra of **4** and **8**. This indicates excimer formation along with ground state aggregation. The photo-stability of the NDI-AA **8**: NDI-TT **4** mixture was also investigated and there was no change in spectral shape and intensity even after 70 min (see Fig. 7).

Hydrogen bonding is sensitive to temperature. We analyzed absorption spectra of NDI-AA **8**, NDI-TT **4** and the NDI-AA **8**: NDI-TT **4** mixture at temperatures between 20 °C and 80 °C in 60:40% DMSO:water to gain greater insight into the interaction between **8** and **4**. As seen in Fig. 8, an increase in temperature decreased the absorbance of NDI-AA **8**. The decrease in absorbance of **8** with increasing temperature could be explained based on the fact that at elevated temperature, hydrogen bonding between adenine and adenine is disrupted, thus, encouraging π-σ interaction among NDIAAs. On the other hand, no such change for NDI-TT **4** with increasing temperature indicates hydrogen bonding is not playing a crucial role in this

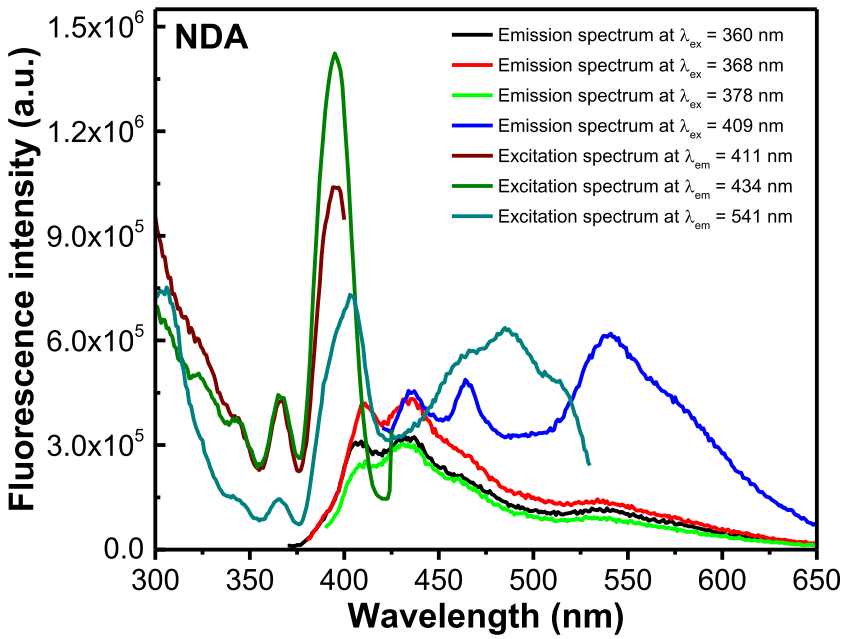

Fig. 5 Fluorescence excitation and emission spectra of NDI-AA **8** in different excitation and emission wavelengths in 60:40 DMSO/water mixture

derivative. This is further supported by Fig. 3a, which showed a decrease in absorbance with a greater water percentage in DMSO. The addition of water does not appear to help hydrogen bond formation between thymine-thymine, rather increasing polarity of the solvent encourages π-σ interaction among NDI-TTs, thus, decreasing the absorbance. A mixture of **4** and **8** led to a decrease in absorbance with elevating temperature but it was less than NDI-AA **8** alone, which is mainly due to the contribution from NDI-AA **8** in the mixture.

Fluorescence spectral change with solvent environment of NDI-AA **8** (Fig. 9) vs. NDI-TT **4** (Fig. 10) was investigated. In NDI-AA **8**, an increase in water content shifted the fluorescence emission spectral position to the blue region and the fluorescence emission peak at around 535 nm disappeared in above 70% water in the solvent mixture. In this case a new peak around 390 nm and a maximum at 405 nm appeared at the expense of the peak at around 475 nm and 550 nm. This 405 nm peak is similar to the spectral position found in the excitation spectrum, which could be 0–0

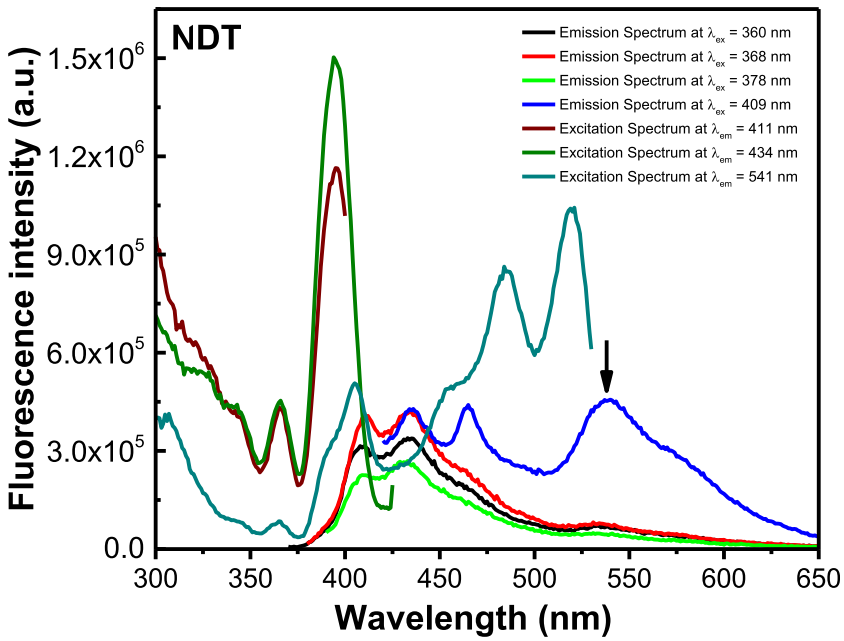

Fig. 6 Fluorescence excitation and emission spectra of NDI-TT **4** in different excitation and emission wavelengths in 60:40 DMSO:water

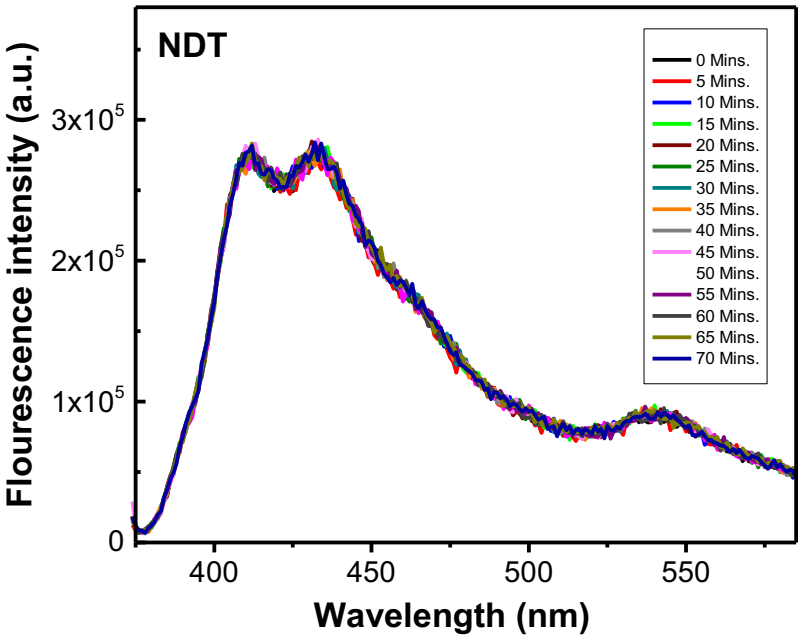

Fig. 7 Fluorescence emission spectra of NDI-TT **4** in 60:40 DMSO:water at different time intervals

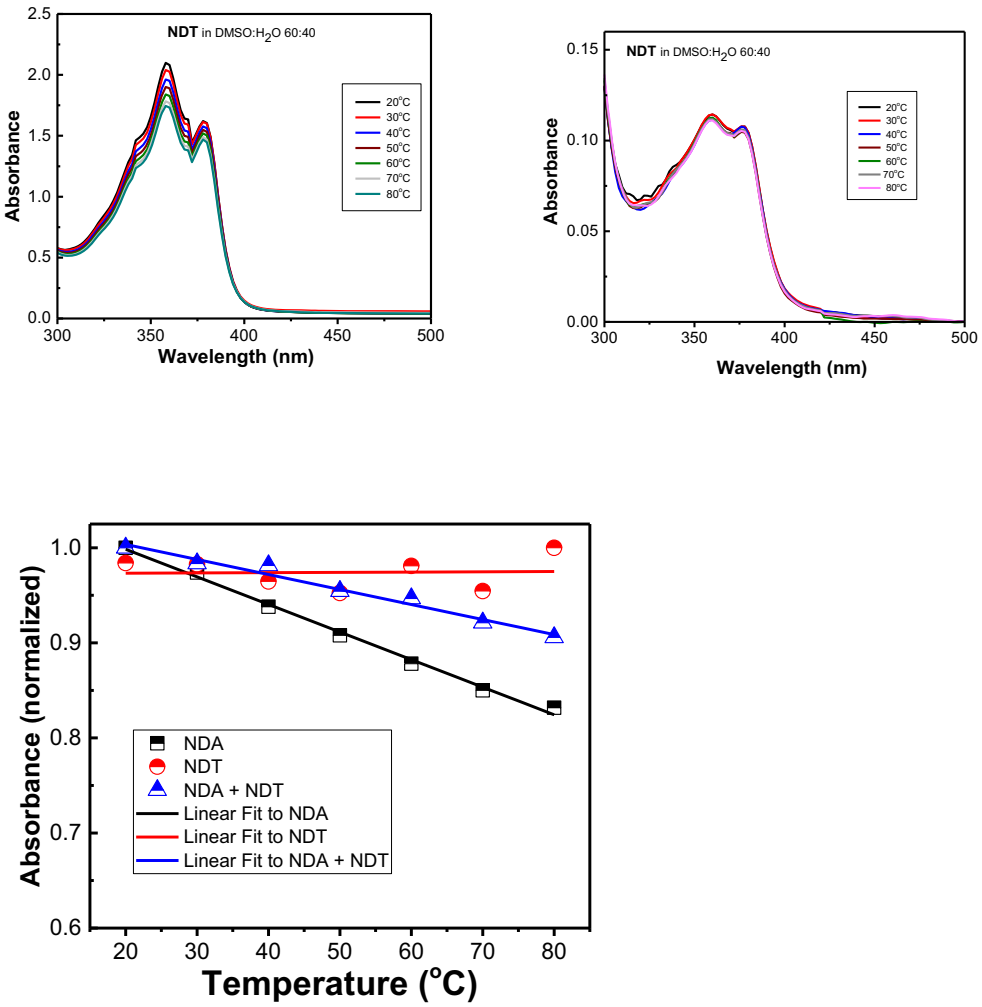

Fig. 8 Fluorescence excitation and emission spectra of NDI-AA **8** in different combination of excitation and emission wavelengths in 60:40 DMSO:water

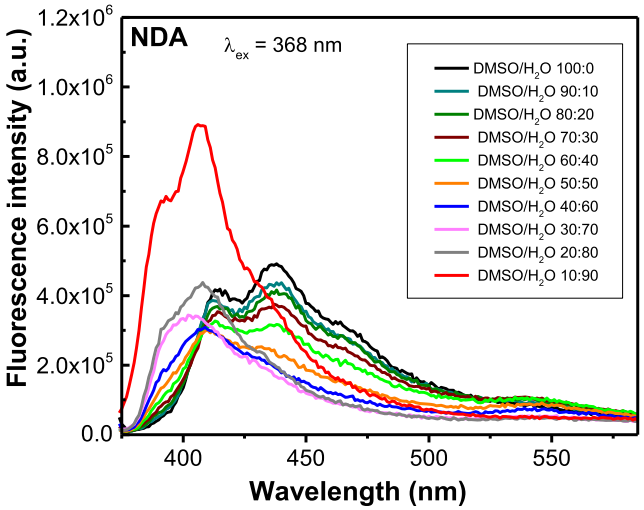

Fig. 9 Fluorescence emission spectra of NDI-AA **8** with increase concentration of water in DMSO/water solvent mixture

transition of NDI-AA **8**. Thus, the emission band around 475 nm and above is due to aggregation resulting from π-σ interaction of NDI-AA **8**. As the water content in the solvent mixture increases, aggregation of NDI-AA **8** is discouraged due to adenine-adenine hydrogen bonding similar to results described earlier. At the same time, the emission spectrum of NDI-TT **4** did not shift to the blue region and the intensity of the peak around 535 nm increased with the expense of fluorescence in 411 nm. In the case of NDI-TT **4**, increasing water content in the solvent mixture facilitates aggregation through π-σ interaction as thymine-thymine hydrogen bonding is less pronounced.

Conclusion

A straightforward, facile and high-yielding strategy, synthesis of nucleobase (adenine/thymine) conjugated naphthalenediimide (NDI), namely, NDI-AA**8** and NDI-TT **4**, was presented. The prepared compounds were characterized by various spectroscopic and analytical techniques. Photophysical study established that NDI-AA **8**, NDI-TT **4** and the NDI-AA **8**: NDI-TT **4** mixture have similar UV-visible absorption in the 300–400 nm region. It was observed that effect of adenine/thymine group on the absorption of the NDI chromophore is negligible and the absorption is due to π-π* transitions of NDI chromophores polarized along the z-axis. The influence of solvent polarity and temperature on absorption spectra suggested aggregation formation, which can be either through intermolecular π-σ interaction between the main chromophore or through intermolecular hydrogen bonding between adenine-adenine groups in NDI-AA **8**. However, addition of water does not help for hydrogen bond formation between thymine-thymine in NDI-TT **4**; rather an increase in solvent polarity encourages π-σ interaction among NDI-TTs. No spectral change for NDI-TT **4** with increasing temperature confirmed hydrogen bonding is not playing a crucial role in NDI-TT **4**. A fluorescence study on NDI-AA **8** indicated excimer formation along with ground state aggregation. It was shown that the emission band around 475 nm and above is due to aggregation resulting from π-σ interaction of NDI-AA **8**. As the water content in the solvent mixture increased, aggregation of **8** was discouraged due to adenine-adenine hydrogen bonding. Nevertheless, the emission spectrum of NDI-TT **4** did not shift to the short wavelength region and the fluorescence intensity of the peak around

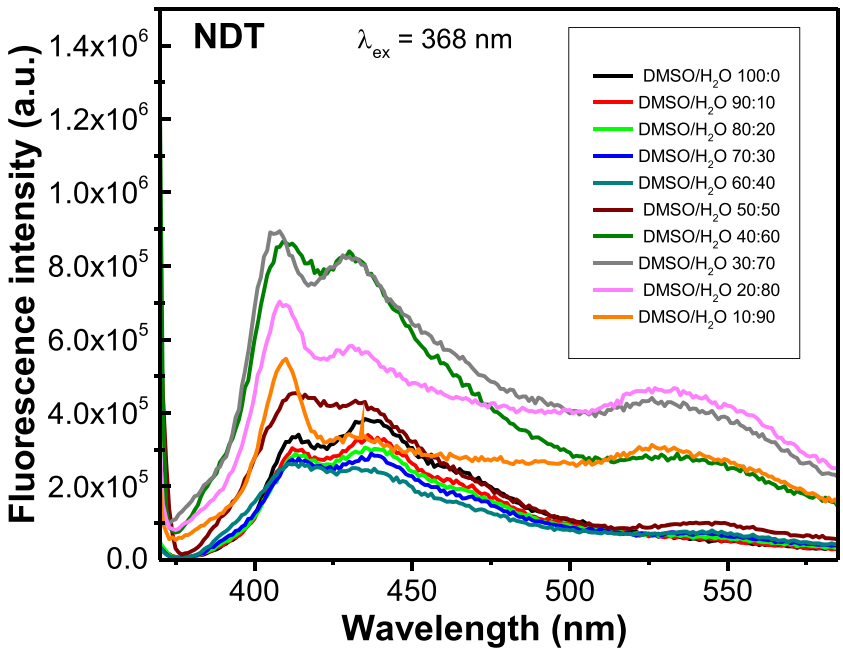

Fig. 10 Fluorescence emission spectra of NDI-TT **4** with increase concentration of water in DMSO/water solvent mixture

535 nm increased at the expense of fluorescence in 411 nm. Thus, an increase in water content in the solvent mixture facilitates aggregation through π-σ interaction in NDI-TT **4**, as thymine-thymine hydrogen bonding is less pronounced. The photo-stability of the NDI-AA **8**: NDI-TT **4** mixture was further established as there was no change in spectral shape and intensity even after 70 min.

Acknowledgements The authors are grateful to the Lebanese National Council for Scientific Research (LNCSR), the University Research Board (URB) and the Kamal Shair CRSL research fund at the American University of Beirut for financial support.

References

1. Bhosale SV, Jani CH, Langford SJ (2008) Chemistry of naphthalene diimides. Chem Soc Rev 37(2):331–342
2. Vollmann H, Becker H, Corell M, Streeck H (1937) Beiträge zur Kenntnis des Pyrens und seiner Derivate. Justus Liebig's Ann der Chemie 531(1):1–159
3. Fallon GD, Lee MA-P, Langford SJ, Nichols PJ (2004) Unusual solid-state behavior in a neutral [2]catenane bearing a hydrolyzable component. Org Lett 6(5):655–658
4. Hansen JG, Feeder N, Hamilton DG, Gunter MJ, Becher J, Sanders JKM (2000) Macrocyclization and molecular interlocking via Mitsunobu Alkylation: highlighting the role of C−H···O interactions in templating. Org Lett 2(4):449–452
5. Vicic DA, Odom DT, Núñez ME, Gianolio DA, McLaughlin LW, Barton JK (2000) Oxidative repair of a thymine dimer in DNA from a distance by a covalently linked organic intercalator. J Am Chem Soc 122(36):8603–8611
6. Mukhopadhyay P, Iwashita Y, Shirakawa M, Kawano S, Fujita N, Shinkai S (2006) Spontaneous colorimetric sensing of the positional isomers of dihydroxynaphthalene in a 1D organogel matrix. Angew Chem Int Ed 45(10):1592–1595
7. Takenaka S, Yamashita K, Takagi M, Uto Y, Kondo H (2000) DNA sensing on a DNA probe-modified electrode using ferrocenylnaphthalene Diimide as the electrochemically active ligand. Anal Chem 72(6):1334–1341
8. Lee HN, Xu Z, Kim SK, Swamy KMK, Kim Y, Kim S-J, Yoon J (2007) Pyrophosphate-selective fluorescent chemosensor at physiological pH: formation of a unique excimer upon addition of pyrophosphate. J Am Chem Soc 129(13):3828–3829
9. Katz HE, Lovinger AJ, Johnson J, Kloc C, Siegrist T, Li W, Lin Y-Y, Dodabalapur A (2000) A soluble and air-stable organic semiconductor with high electron mobility. Nature 404:478–481
10. Brochsztain S, Rodrigues MA, Demets GJF, Politi MJ (2002) Stabilization of naphthalene-1,8:4,5-dicarboximide radicals in zirconium phosphonate solid materials and thin films. J Mater Chem 12(5):1250–1255
11. Stewart WW (1981) Lucifer dyes—highly fluorescent dyes for biological tracing. Nature 292:17–21
12. Das A, Molla MR, Ghosh S (2011) Comparative self-assembly studies and self-sorting of two structurally isomeric naphthalenediimide (NDI)-gelators. J Chem Sci 123(6):963–973
13. Würthner F, Ahmed S, Thalacker C, Debaerdemaeker T (2002) Core-substituted naphthalene bisimides: new fluorophors with tunable emission wavelength for FRET studies. Chem - A Eur J 8(20):4742–4750
14. Narayanaswamy N, Avinash MB, Govindaraju T (2013) Exploring hydrogen bonding and weak aromatic interactions induced assembly of adenine and thymine functionalised naphthalenediimides. New J Chem 37(5):1302
15. Das A, Ghosh S (2016) H-bonding directed programmed supramolecular assembly of naphthalene-diimide (NDI) derivatives. Chem Commun 52(42):6860–6872
16. Hammud H, El-Dakdouki M, Sonji N, Bouhadir K (2010) Solvatochromic absorption and fluorescence studies of adenine, thymine and uracil thio-derived acyclonucleosides. Eur J Chem 1(2):325
17. Bouhadir KH, Koubeissi A, Mohsen FA, El-Harakeh MD, Cheaib R, Younes J, Azzi G, Eid AA (2016) Novel carbocyclic nucleoside analogs suppress glomerular mesangial cells proliferation and matrix protein accumulation through ROS-dependent mechanism in the diabetic milieu. II. Acylhydrazone-functionalized pyrimidines. Bioorg Med Chem Lett 26(3):1020–1024